HHS Public Access

Author manuscript

Neuropharmacology. Author manuscript; available in PMC 2022 March 01.

Published in final edited form as:

Neuropharmacology. 2021 March 01; 185: 108456. doi:10.1016/j.neuropharm.2021.108456.

Kappa opioid receptor activation in the amygdala disinhibits CRF neurons to generate pain-like behaviors.

Matthew Hein[a,1], **Guangchen Ji**[a,b,1], **Dalton Tidwell**[a], **Preston D'Souza**[a], **Takaki Kiritoshi**[a], **Vadim Yakhnitsa**[a], **Edita Navratilova**[c], **Frank Porreca**[c], **Volker Neugebauer**[a,b,d]

[a]Department of Pharmacology and Neuroscience, Texas Tech University Health Sciences Center, Lubbock, TX, USA

[b]Center of Excellence for Translational Neuroscience and Therapeutics, Texas Tech University Health Sciences Center, Lubbock, TX, USA

[c]Department of Pharmacology, Arizona Health Sciences Center, University of Arizona, Tucson, AZ, USA

[d]Garrison Institute on Aging, Texas Tech University Health Sciences Center, Lubbock, TX, USA

Abstract

Recent evidence suggests that kappa opioid receptors (KOR) in limbic brain regions such as the amygdala contribute to pain conditions, but underlying mechanisms remain to be determined. The amygdala is an important player in averse-affective aspects of pain and pain modulation. The central nucleus (CeA) serves output functions through projection neurons that include corticotropin releasing factor (CRF) expressing neurons. The CeA is also rich in KOR. Here we tested the novel hypothesis that KOR activation in the CeA generates pain-like behaviors through a mechanism that involves inhibition of synaptic inhibition (disinhibition) of CRF neurons. Intra-CeA administration of a KOR agonist (U-69,593) increased vocalizations of naïve rats to noxious stimuli, and induced anxiety-like behaviors in the open field test (OFT) and avoidance in the conditioned place preference test, without affecting mechanosensory thresholds. Optogenetic silencing of CeA-CRF neurons blocked the facilitatory effects of systemically applied U-69,593 in naïve rats. Patch-clamp recordings of CRF neurons in rat brain slices found that U-69,593 decreased feedforward inhibitory transmission evoked by optogenetic stimulation of parabrachial afferents, but had no effect on monosynaptic excitatory transmission. U-69,593 decreased frequency, but not amplitude, of inhibitory synaptic currents, suggesting a presynaptic action.

Corresponding author: Volker Neugebauer, M.D., Ph.D., 3601 4th St, MS 6592, Department of Pharmacology and Neuroscience, Texas Tech University Health Sciences Center, Lubbock, TX, 79430, USA. volker.neugebauer@ttuhsc.edu.

Matthew Hein: Methodology, Investigation, Visualization, Writing – Original Draft. **Guangchen Ji:** Conceptualization, Supervision, Methodology, Investigation, Visualization, Writing – Original Draft, Funding acquisition. **Dalton Tidwell:** Investigation, Visualization. **Preston D'Souza:** Investigation, Visualization. **Takaki Kiritoshi:** Validation, Investigation, Visualization. **Vadim Yakhnitsa:** Validation, Investigation, Visualization. **Edita Navratilova:** Conceptualization, Methodology, Writing – Review & Editing, Funding acquisition. **Frank Porreca:** Conceptualization, Methodology, Writing – Review & Editing, Funding acquisition. **Volker Neugebauer:** Conceptualization, Methodology, Supervision, Visualization, Writing – Review & Editing, Project administration, Funding acquisition

[1]These authors contributed equally

Multiphoton imaging of CeA-CRF neurons in rat brain slices showed that U-69,593 increased calcium signals evoked by electrical stimulation of presumed parabrachial input. This study shows for the first time that KOR activation increases activity of amygdala CRF neurons through synaptic disinhibition, resulting in averse-affective pain-like behaviors. Blocking KOR receptors may therefore represent a novel therapeutic strategy.

Keywords

Amygdala; pain; corticotropin-releasing factor; kappa opioid receptor; patch clamp; behavior

1. Introduction

The better understanding of mechanisms underlying opioid and opioid receptor functions is required for the development of new and improved therapeutics. While mu-opioid receptors typically mediate analgesic effects, kappa opioid receptors have been linked to aversiveness as well as anxiety and stress responses through actions in limbic brain regions such as the amygdala (Bruchas et al., 2010; Crowley et al., 2016; Gilpin et al., 2014; Lalanne et al., 2014; Land et al., 2008; Smith et al., 2012; Tejeda et al., 2017). The amygdala plays an important role in emotional-affective aspects of behaviors, stress integration, and stress-related disorders as well as in averse-affective aspects of pain and pain modulation (Neugebauer et al., 2004; Thompson and Neugebauer, 2019). The amygdala receives pain-related information from the brainstem parabrachial area, which targets the central amygdala (CeA) directly, and from thalamo-cortical regions, which project to the lateral-basolateral amygdala (LA-BLA) circuity. Neuroplasticity in BLA and CeA has been linked to pain-like behaviors in different pain conditions (Allen et al., 2020; Corder et al., 2019; Neugebauer, 2020; Neugebauer et al., 2004; Thompson and Neugebauer, 2019; Wilson et al., 2019).

The amygdala is one of the brain areas with particularly high expression of KOR based on radioligand binding, immunohistochemistry and in situ hybridization (Cahill et al., 2014; Le Merrer et al., 2009; Mansour et al., 1996; Mansour et al., 1995). Dynorphin, considered the endogenous ligand for KOR (Bruchas et al., 2010), is synthesized primarily in neurons in the lateral CeA (CeL) (Marchant et al., 2007), and one third of these neurons co-express corticotropin-releasing factor (Marchant et al., 2007). Conversely, a majority of CRF neurons co-express prodynorphin (Pomrenze et al., 2015). CRF neurons receive peptidergic input from the parabrachial area (Harrigan et al., 1994) and form long range projections to extra-amygdalar targets to promote aversive and anxiety-like behaviors (Beckerman et al., 2013; Fendt et al., 1997; Marcilhac and Siaud, 1997; McCall et al., 2015; Pomrenze et al., 2019; Pomrenze et al., 2015; Reyes et al., 2011), suggesting that CRF neurons serve amygdala input-output functions.

While KOR function has been studied in the CeA before, and KOR in the CeA has been implicated in pain mechanisms, the role of KOR in modulating amygdala CRF neurons, their parabrachial input and dependent pain-related behaviors remains to be determined and was addressed here. Previous studies found that administration of a KOR antagonist (nor-BNI) into the CeA blocked stress-induced mechanical hypersensitivity in a priming model of

medication overuse headache (Xie et al., 2017) and prevented conditioned place preference (CPP) to gabapentin but had no significant effect on mechanosensitivity in a neuropathic pain model (spinal nerve ligation, SNL), suggesting that nor-BNI eliminated the aversive qualities of ongoing pain but not sensory aspects of pain (Navratilova et al., 2019). Nor-BNI administered into the CeA also restored the loss of diffuse noxious inhibitory control (DNIC) in the SNL model, which is consistent with a role of KOR in enhanced descending facilitation in pain conditions. The effects of KOR antagonists in these studies were lateralized to the right CeA. KOR blockade in the CeA had no effect under control conditions in the absence of injury or sensitization (Phelps et al., 2019; Xie et al., 2017). The functional change of KOR signaling could be the result of increased dynorphin release and increased phosphorylation of KOR (Xie et al., 2017).

Brain slice physiology studies showed that the inhibitory effects of nor-BNI in a neuropathic pain model (SNL) involved increased synaptic inhibition of CeL neurons (Navratilova et al., 2019). Conversely, U-69,593 decreased synaptic inhibition of medial CeA neurons through a presynaptic action (Gilpin et al., 2014; Kang-Park et al., 2013) but also produced an outward current in medial CeA neurons, indicative of a postsynaptic inhibitory effect (Chieng et al., 2006; Zhu and Pan, 2004).

Opioid receptors generally couple to inhibitory Gi/o-proteins (Standifer and Pasternak, 1997). Here we tested the novel hypothesis that KOR activation increases activity of CeA-CRF neurons through inhibition of synaptic inhibition (dis-inhibition) driven by parabrachial input to the CeA. Specifically, KOR inhibit the inhibitory element of this feedforward inhibition. Additionally, we sought to determine the contribution of CeA-CRF neurons to the behavioral consequences of KOR activation.

2. Materials and Methods

2.1 Animals

Male, hemizygous transgenic and wildtype Crh-Cre rats on Wistar background (Pomrenze et al., 2015) (initial breeding pairs kindly provided by Dr. Robert Messing, UT Austin), 250 g to 350 g (2–3-month-old) at time of testing, were housed 3 per cage on a 12-hour light-dark cycle (lights on at 7:00 am) with unrestricted access to food and water. These Crh-Cre rats allow the visualization and targeting of CRF neurons (Pomrenze et al., 2015). Please note that Crh stands for corticotropin releasing hormone, which is the same as corticotropin releasing factor (CRF). On the day of the experiment, animals were transferred from the animal facility to the laboratory and acclimated for at least 1 h. All procedures were approved by the Institutional Animal Care and Use Committees (IACUC) of Texas Tech University Health Sciences Center. All studies were conducted in accordance with the policies and recommendations of the National Institutes of Health Guide for the Care and Use of Laboratory Animals. Experiments were done in a blinded fashion and reproduced by several investigators.

2.2 Experimental protocol

The effect of a selective kappa opioid receptor (KOR) agonist (U-69,593) (Zhou et al., 2013) compared to vehicle control was tested in behavioral and electrophysiological experiments. In behavioral experiments, stereotaxic drug application into the central nucleus of the amygdala (CeA) or offsite (striatum) by microdialysis was used, and a guide cannula was implanted the day before (see 2.3). Behavioral assays were done 15 min after starting stereotaxic drug application (see Behaviors). In some experiments, the effect of optogenetic silencing of CeA-CRF neurons was tested on the effects of a systemically applied KOR agonist. A viral vector (see 2.4) was injected stereotaxically into the CeA 4–5 weeks before behavioral testing to express halorhodopsin (eNpHR3.0) in CeA-CRF neurons (see 2.4). In brain slice physiology experiments, KOR agonist or ACSF was applied to the brain slice by gravity-driven superfusion. For optogenetic stimulation of parabrachial afferents to the CeA, a viral vector was injected stereotaxically into the parabrachial area to express channelrhodopsin (ChR2) in glutamatergic parabrachial neurons (see 2.4). All drug applications and recordings were done in the right CeA because of evidence for hemispherical lateralization of KOR signaling to the right CeA (Nation et al., 2018; Navratilova et al., 2020; Phelps et al., 2019).

2.3 Drug application in awake animals

For stereotaxic drug administration into the CeA by microdialysis, animals were anesthetized with isoflurane (5%, induction; 2%, maintenance; precision vaporizer, Harvard Apparatus, Holliston, MA) and placed in a stereotaxic frame (David Kopf Instruments, Tujunga, CA). For drug applications into the CeA, a guide cannula (CMA/Microdialysis, Solna, Sweden) was implanted stereotaxically into the right CeA the day before the experiment using the following coordinates (Paxinos and Watson, 1998): 2.5 mm caudal to bregma, 4.0 mm lateral to midline, and 7.0 mm deep. For offsite controls, the striatum dorsolateral to CeA was targeted using the following coordinates (Paxinos and Watson, 1998): 2.0 mm caudal to bregma, 4.5 mm lateral to midline, and 6.0 mm deep, as in our previous studies (Fu et al., 2008; Kim et al., 2017), because it is adjacent to CeA but does not project to CeA. The cannula was fixed to the skull with dental acrylic (Plastic One, Roanoke, VA). Antibiotic ointment (Bacitracin) was applied to prevent infection. On the day of the experiment, a microdialysis probe (CMA/Microdialysis 11) protruding 1 mm from the guide cannula was inserted and connected to an infusion pump (Harvard Apparatus) with polyethylene tubing. U-69,593 (Sigma-Aldrich, St. Louis, MO) or artificial cerebrospinal fluid (ACSF; in mM: 117 NaCl, 4.7 KCl, 1.2 NaH_2PO_4, 2.5 $CaCl_2$, 1.2 $MgCl_2$, 25 $NaHCO_3$, and 11 glucose) was administered for 30–40 min at 5 μl/min. U-69,953 stock solution was diluted in ACSF to the final concentration (100 μM), which is 100-fold higher than the intended target concentration in the tissue due to the concentration gradient across the dialysis membrane and diffusion in the brain tissue (Fu and Neugebauer, 2008; Kiritoshi et al., 2016; Li et al., 2011; Ren et al., 2013; Thompson et al., 2018). In some experiments, U-69,593 (in sterile saline) was applied systemically (1.0 mg/kg, intraperitoneally, i.p.).

2.4 Optogenetics

2.4.1 Behavior.—For optical silencing of CeA-CRF neurons in behavioral experiments, a cre-dependent DIO (double inverted open reading frame) viral vector (1 μl, 10^{12} units / 100 μl; packaged by the vector core facility at the University of North Carolina, Chapel Hill, NC) expressing halorhodopsin in CRF neurons (rAAV5/EF1a-DIO-eNpHR3.0-eYFP) were injected into the lateral CeA (CeL) using a 5 μl Hamilton syringe (33 gauge) while the animals were anesthetized with isoflurane (5%, induction; 2%, maintenance; precision vaporizer, Harvard Apparatus, Holliston, MA) and placed in a stereotaxic frame (David Kopf Instruments, Tujunga, CA). 4–5 weeks were allowed for vector expression before the experiments. Coordinates were as follows (Paxinos and Watson, 1998): CeA, 2.5 mm caudal to bregma, 4.0 mm lateral to midline, and 7.5 mm deep. For optical stimulation in behavioral experiments, a wireless system (Teleopto, Amuza, San Diego, CA) was used that consisted of a headstage with LED light source and receiver, implantable optical fiber (200 μm, diameter), remote controller and pulse generator. The optical fiber was implanted into the CeA the day before the behavioral testing while the animal was anesthetized with isoflurane (5%, induction; 2%, maintenance), using a similar procedure as for implantation of the microdialysis probe (see 2.3). Optical stimulation (590 nm for eNpHR3.0; 473 nm as control; 5 ms, 20 Hz, 5 mW) started 5 min before behavioral testing and continued during testing. The parameters for optogenetic stimulation in our study were similar to those used by others to silence CeA-CRF (De Guglielmo et al., 2019).

2.4.2 Electrophysiology.—For optical activation of parabrachial afferents to CeA neurons in brain slice experiments, viral vectors (1 μl, 10^{12} units / 100 μl; vector core facility, University of North Carolina) expressing channelrhodopsin 2 (ChR2) in glutamatergic neurons of the parabrachial nucleus (rAAV5-CaMKIIa-hChR2(H134R)-eYFP) were injected into the external lateral parabrachial nucleus using a 5 μl Hamilton syringe (33 gauge). 4–5 weeks were allowed for vector expression before the experiments. Coordinates were as follows (Paxinos and Watson, 1998): parabrachial nucleus, 6.6–6.5 mm caudal to bregma, 2.2–2.3 lateral, 7.4–7.1 mm deep at a 15-degree anteroposterior angle. For optical stimulation in brain slice experiments, blue (470 ± 20 nm) or yellow (585 ± 10 nm) light was generated by a broad spectrum LED illumination system (X-Cite Xylis, Excelitas Technologies Corp., Waltham, MA) by passing through an ET470/40x (blue light, Chroma Technology Corp., Bellows Falls, VT) or ET585/20m (yellow light, Chroma Technology Corp.) filter and through the objective of the microscope (BX51, Olympus, Waltham, MA) with an integrated LED stimulation system (X-Cite XYLIS). Blue light was used to activate ChR2 expressing parabrachial fiber terminals (Sugimura et al., 2016) whereas yellow light served as control (10 ms, 0.05 Hz; 5–10 mW).

2.5 Histological verification of drug administration and injection sites

Locations of the tips of the microdialysis probes and injection sites of viral vectors were verified histologically post-mortem (see Fig. 1B and C). Rats were euthanized with FATAL-plus (pentobarbital sodium, 125 mg/kg, intravenously) followed by decapitation using a small guillotine (Harvard Apparatus Decapitator). Brains were fixated in 4% paraformaldehyde, transferred to 30% sucrose in 0.1 M phosphate buffer, and then embedded in Optimal Cutting Temperature (O.C.T.) compound. Frozen coronal sections 30

μm were cut at −20 °C using a cryostat (Vibratome UltraPro 5000) and analyzed under the microscope. Confocal microscopy (FV3000, Olympus, Center Valley, PA) was used to identify CRF neurons expressing halorhodopsin (Fig. 1A), eYFP in the CeA (Fig. 1B), and ChR2 expression in the CeA (Fig. 1E) and parabrachial nucleus (Fig. 1F). Location was verified with reference to the Paxinos and Watson brain atlas (Paxinos and Watson, 1998).

2.6 Behaviors

2.6.1 Vocalizations.—Vocalizations in the audible (20 Hz-16 kHz) and ultrasonic (25±4 kHz) ranges were measured as in our previous studies (Han et al., 2005; Kiritoshi et al., 2016; Mazzitelli and Neugebauer, 2019; Neugebauer et al., 2007; Thompson et al., 2015). Animals were briefly anesthetized with isoflurane (5%) and placed in a custom designed recording chamber (U.S. Patent 7,213,538). After habituation to the chamber for 30 min, vocalizations were evoked by brief (15 s) innocuous (500 g / 30 mm^2) and noxious (1500 g / 30 mm^2) stimuli applied to the left knee joint or hindpaw, using a calibrated forceps equipped with a force transducer whose output was displayed in grams on an LED screen. A condenser microphone connected to a preamplifier and a bat detector were used to measure audible (< 16 kHz) and ultrasonic (25 kHz) vocalizations, respectively. The sound detectors were connected to a filter and amplifier (UltraVox four-channel system; Noldus Information Technology) to record and analyze number and duration of individual vocalization events in set frequency ranges. Vocalizations were recorded for 1 min and analyzed using Ultravox 2.0 software (Noldus Information Technology, Leesburg, VA).

2.6.2 Mechanosensory thresholds.—Hindlimb withdrawal thresholds were evaluated after the vocalization measurements while the rat was in the recording chamber. A calibrated forceps with force transducer (see 2.6.1) was used to compress the left knee joint or hindpaw with continuously increasing intensity until a reflex response was evoked. The average value from 2–3 trials was used to calculate the mechanical threshold, i.e., the force required to evoke a reflex response.

2.6.3 Open field test (OFT).—OFT was used to measure exploration of the peripheral and central zones of an arena (70 cm × 70 cm) with acrylic walls (45 cm high) for 15 min with a computerized videotracking and analysis system (EthoVision XT 11, Noldus Information Technology) as described previously (Ji et al., 2018). Number of entries (frequency) and time spent in the center field (35 cm × 35 cm) were calculated for the first 5 min. Avoidance of the center field is interpreted to suggest anxiety-like behavior.

2.6.4 Conditioned place preference (CPP).—The test apparatus consisted of two chambers (30×30×40 cm each) with distinguishing features (walls with different patterns of black and white stripes, laminate floors with slightly different textures and different grey tones), a neutral zone (corridor), and a computerized analysis system (Opto-Max software, Columbus instruments, Columbus, OH) that measured the movements of the animal between and within the chambers based on disruption of infrared beams. We followed the experimental protocol described in our previous studies (Ji et al., 2015), which is similar to (King et al., 2009). After pre-conditioning baseline measurements (3 days; to rule out any chamber preference) rats received vehicle paired with one chamber as control, and drug

treatment (U-69,593; see 2.3) paired with the opposite chamber 4 h later (conditioning phase). Rats were confined to the appropriate chamber for 30 min. Chamber pairings were counterbalanced. Rats showing a pre-test preference of >60% were excluded from the study. The following day (test day), rats were placed in the CPP box with access to both chambers, and behavior was recorded for 15 min while the time spent in each chamber was recorded. Difference scores were calculated as the time spent in the drug or vehicle paired chamber on test day minus time spent in the same chamber on preconditioning day.

2.7 Brain slice electrophysiology and calcium imaging

2.7.1 Brain slice preparation.—Coronal (400 μm) brain slices containing the CeA of the right hemisphere were obtained as described previously (Navratilova et al., 2019; Thompson et al., 2018). The right hemisphere was selected because of evidence for lateralized amygdala function in pain (see 2.2 and (Carrasquillo and Gereau, 2008; Ji and Neugebauer, 2009; Kolber et al., 2010; Nation et al., 2018; Navratilova et al., 2020; Phelps et al., 2019)). After immersing the brains in oxygenated ice-cold sucrose-based physiological solution (87 NaCl, 75 sucrose, 25 glucose, 5 KCl, 21 $MgCl_2$, 0.5 $CaCl_2$, and 1.25 NaH_2PO_4), brain slices were prepared using a Vibratome (VT1200S, Leica Biosystems, Nussloch, Germany). Brain slices were then incubated in oxygenated ACSF (see 2.3) at 35°C for at least 1 h before being transferred to the recording chamber and superfused by ACSF (35°C) at ~2 ml/min. Only one or two brain slices per animal were used. Only one neuron was recorded in each slice.

2.7.2 Identification and recording of CRF neurons.—To visualize CRF neurons in the CeA, rats were injected with AAV5-EF1α-DIO-mCherry into the right CeA 4–5 weeks before brain slices were obtained to allow for viral vector expression (Fig. 1D). Whole-cell voltage- and current-clamp recordings were then made from visually identified CRF neurons in the CeL using DIC-IR videomicroscopy and fluorescence illumination (BX51, Olympus, Waltham, MA) as described previously (Navratilova et al., 2019; Thompson et al., 2018). mCherry-expressing CRF neurons were visualized using an LED illumination system (X-Cite Xylis, see 2.4.2) and an ET-DSRed filter set (49005, excitation: 545 ± 15 nm, ET545/30x; emission: 620 ± 30 nm, ET620/60m; T570lp dichroic mirror, Chroma Technology Corp., Bellows Falls, VT). Borosilicate glass recording electrodes had tip resistances of 3–6 MΩ and were filled with a potassium gluconate based internal solution containing (in mM): 122 K-gluconate, 5 NaCl, 0.3 $CaCl_2$, 2 $MgCl_2$, 1 EGTA, 10 HEPES, 5 Na_2-ATP, and 0.4 Na_3-GTP; pH was adjusted to 7.2–7.3 with KOH and osmolarity to 280 mOsm/kg with sucrose. Data acquisition and analysis was done using a low-noise Digidata 1440A interface (Axon Instruments, Molecular Devices, San Jose, CA), a dual 4-pole Bessel filter (Warner Instruments, Hamden, CT), Axoclamp-2A amplifier (Axon Instruments), and pClamp10 software (Axon Instruments). If series resistance (monitored with pClamp10 software) changed >20%, the neuron was discarded.

2.7.3 Electrophysiology outcome measures.—Action potentials were evoked in current clamp from a holding potential of −60 mV using 0.5 s depolarizing current steps of increasing amplitude. Synaptic transmission was measured in voltage clamp. Monosynaptic excitatory postsynaptic currents (EPSCs) and glutamate-driven inhibitory postsynaptic

currents (IPSCs) were evoked in CRF neurons by focal optical stimulation (473 nm for ChR2 activation) of terminals of parabrachial neurons (see 2.4.2 and Fig. 1E,F), similarly to our previous study on optically evoked synaptic responses of CeA neurons (Kiritoshi and Neugebauer, 2018). EPSCs were recorded at −70 mV and could be blocked by antagonists for NMDA receptors (DL-2-amino-5-phosphonopentanoic acid, AP5, 50 μM) and non-NMDA receptors (6-cyano-7-nitroquinoxaline-2,3-dione, CNQX, 20 μM). IPSCs were recorded at 0 mV and were blocked by a $GABA_A$ receptor antagonist (bicuculline, 10 μM) and by CNQX, consistent with glutamate-driven feedforward inhibition (Ren et al., 2013). Spontaneous and miniature (in tetrodotoxin citrate, TTX, 1 μM) IPSCs were recorded at 0 mV as described previously (Kiritoshi and Neugebauer, 2015) to assess pre- versus post-synaptic mechanisms. A fixed length of traces (5 min) was analyzed for frequency and amplitude distributions using MiniAnalysis program 6.0.7 (Synaptosoft, Decatur, GA). Detection threshold for an event was set to 4 times the root mean square (RMS) value, and peaks were detected automatically, but each detected event was also visually inspected. Spontaneous and miniature IPSCs were measured 5–10 min before and 10–15 min during drug application. All drugs were purchased from Tocris Bioscience, Bio-Techne Corporation, Minneapolis, MN).

2.7.4 Calcium imaging.—To measure calcium signals in CeA-CRF neurons, rats were injected with AAV5-Syn-Flex-GCaMP6f into the right CeA 4 weeks before brain slices were obtained to allow viral vector mediated expression of a fluorescent calcium sensor. Brain slices were incubated in oxygenated ACSF at 35°C for at least 1 h before being transferred to the recording chamber and superfused by ACSF (35°C) at ~2 ml/min as in the electrophysiology experiments (2.7.1). A multiphoton system (Intelligent Imaging Innovations, Inc, 3i, Denver, CO) equipped with a VIVO™ 2-Photon 200 Microscopy Workstation was used to record calcium transient evoked by electrical stimulation (mA; 500 μs; 0.05 Hz) of the dorsomedial fiber tract containing presumed axons from the parabrachial area (Ikeda et al., 2007; Neugebauer et al., 2003). The 2-photon (2P) excitation light was generated by a mode-locked Ti:Sapphire laser (920 nm, model Mai-Tai DeepSee, Spectra-Physics, Santa Clara, CA, USA). A 20x/1.0NA water-immersion lens (Zeiss, Germany) was used for imaging of neuron clusters. Images were acquired at a rate of 0.85 frames/s with a resolution of 512 × 512 pixels, corresponding to an image plane of 350 × 350 μm. CeA-CRF neurons that responded to electrical stimulus were further analyzed. Fluorescent activity and background ($\Delta F/F_0$) were analyzed using SlideBook 6 (3i, Denver, CO, USA). Responses were recorded 15 minutes before and 30 minutes during drug application, and could be blocked by CNQX, consistent with glutamatergic synaptic drive.

2.8 Statistical Analysis

Statistical significance was accepted at the level $P < 0.05$. All averaged values are presented as means ± SEM. GraphPad Prism 7.0 software (Graph-Pad Software, San Diego, CA) was used for all statistical analyses. One-way ANOVA (repeated measures if appropriate) with Bonferroni post hoc tests was used for multiple comparisons. Paired and unpaired t-tests were used as appropriate for comparison of two sets of data that had Gaussian distribution and similar variance as indicated. Group sizes were determined by power analysis using

pilot data to estimate the effect size to obtain statistical significance at an alpha of 0.05 for a power of 95%.

3. Results

In this study we tested the hypothesis that activation of kappa opioid receptors (KOR) in the amygdala (CeA) with a selective agonist (U-69,593) would generate or enhance pain-related behaviors through a mechanism that involves activation of CeA-CRF neurons through disinhibition. KOR activation would inhibit synaptic inhibition driven by glutamatergic input from the parabrachial nucleus (feedforward inhibition). In the first series of experiments we tested the behavioral effects of U-69,593. Next, we used brain slice physiology and calcium imaging to determine the underlying synaptic mechanisms. The focus was on the right amygdala because of evidence for lateralization of pain modulation (for recent review see Allen et al., 2020) and KOR signaling (Nation et al., 2018; Navratilova et al., 2020; Phelps et al., 2019) to the right CeA.

3.1 Facilitatory behavioral effects of a KOR agonist in the amygdala

Administration of a KOR agonist (U-69,593, 100 μM in microdialysis probe) into the CeA had no significant effect on mechanical withdrawal thresholds (see Materials and Methods; P = 0.0741, paired t-test, n = 12; Fig. 2A) but increased emotional-affective responses (ultrasonic vocalizations evoked by brief noxious compression of the knee or hindpaw; see 2.6.1) significantly (P = 0.0032, paired t-test, n = 14; Fig. 2B). No difference in the effects of U-69,593 was found for stimulation of the knee joint and paw, and therefore the data were pooled. U-69,593 also increased anxiety-like behaviors in the open field test, measured as decreased time spent in the center area and decreased number of entries into the center area (Fig. 2C and D; P = 0.0005 and 0.0016, t-tests; ACSF, n = 10; U-69,593, n = 11). U-69,593 induced significant avoidance for the chamber that was paired with drug treatment in the conditioned place preference (CPP) test (Fig. 2E; P = 0.0466, $F_{3,24}$ = 3.079, ANOVA with Bonferroni posthoc tests, n = 7). U-69,593 paired chamber avoidance is also reflected in the lower difference score (time in paired chamber on test day – time in chamber on pre-test day) for the U-69,593 paired chamber than the vehicle paired chamber (Fig. 2F; P = 0.0350, t-test, n = 7), suggesting induction of averseness as observed in pain conditions (King et al., 2009; Navratilova et al., 2019; Navratilova et al., 2020). The concentration of U-69,593 in the microdialysis probe was 100-fold higher than the intended target concentration in the tissue due to the concentration gradient across the dialysis membrane and diffusion in the brain tissue (see 2.3) (Mazzitelli and Neugebauer, 2019). Importantly, offsite control administration of U-69,593 into the striatum (see 2.3) had no significant effects on mechanical thresholds (P = 0.5110, paired t-test, n = 6), vocalizations (P = 0.3419, paired t-test, n = 6), and anxiety-like behavior (duration, P > 0.9999; entries, P = 0.7968, t-tests, n = 6; Fig. 2A–D).

3.2 Facilitatory behavioral effects of a KOR agonist were blocked by optical silencing of CRF neurons in the amygdala

To determine the contribution of CRF neurons in the CeA to the facilitatory effects of a KOR agonist, we used optogenetic silencing of CRF neurons while the KOR agonist was

applied systemically (Fig. 3). Behavioral testing was done 30 min after application of U-69,953 (1.0 mg/kg, intraperitoneally, i.p.). Fifteen minutes later, optical silencing of CeA-CRF neurons with yellow light to activate halorhodopsin (see 2.4.1) was done for 15 min followed by behavioral testing at the 60 min time point post drug injection. For optogenetic stimulation we used parameters that have been shown before to silence CeA-CRF neurons (De Guglielmo et al., 2019). For time course analysis, mechanosensitivity and vocalizations were tested every 15 min (n = 8 rats). Systemic application of U-69,593 had no significant effect on mechanical withdrawal thresholds compared to predrug controls, and optical silencing of CeA-CRF neurons (see 2.4.1) also had no significant effect ($P > 0.05$, $F = 0.3264$, repeated measures ANOVA, n = 8; Fig. 3A,B). Systemically applied U-69,593 increased emotional-affective responses (ultrasonic vocalizations evoked by brief compression of the knee or hindpaw; see 2.6.1.) significantly ($P < 0.01$, $F = 9.356$, innocuous; $F = 7.28$, noxious; repeated measures ANOVA; results of Bonferroni posthoc tests are indicated in the graphs, n = 8; Fig. 3C), and this effect was blocked by optogenetic silencing of CeA-CRF neurons ($P < 0.05$, repeated measures ANOVA with Bonferroni posthoc test, n = 8; Fig. 3C,D). Similarly, optogenetic silencing of CeA-CRF neurons blocked the significant ($P < 0.05$, $F = 6.204$, duration; $F = 4.609$, frequency; repeated measures ANOVA with Bonferroni posthoc test, n = 8) anxiogenic-like effects of systemically applied U-69,593 in the open-field test ($P < 0.05$, repeated measures ANOVA with Bonferroni posthoc test, n = 6; Fig. 3E,F). Importantly, blue light application as a control had no effect (Fig. 3B,D), and yellow light had no effect on withdrawal thresholds (Fig. 3A,B), arguing against non-specific effects of optical silencing of CRF neurons with yellow light to activate halorhodopsin.

3.3 Inhibitory effects of a KOR agonist on synaptic inhibition increase calcium signaling in CRF neurons

Brain slice electrophysiology was performed to determine the synaptic actions of U-69,593 on CeA-CRF neurons. The hypothesis was that KOR activation would inhibit synaptic inhibition (disinhibition) driven by parabrachial input (feedforward imbibition; see circuitry in (Neugebauer, 2020)). Recordings were made from visually identified CRF neurons in the lateral CeA (Fig. 4A). Synaptic responses were evoked by optical stimulation of ChR2 expressing glutamatergic parabrachial afferents (see 2.4.2 and 2.7.3). We used stimulus parameters that have been shown before to activate CeA neurons (Sugimura et al., 2016). Out of 40 CeA-CRF neurons, 90% responded to optical activation of parabrachial input; both excitatory and inhibitory postsynaptic currents (EPSCs and IPSCs) were evoked in the majority of neurons (31 / 40, 78%). U-69,593 (1 μM, 15 min) decreased IPSCs significantly ($P < 0.001$, paired t-test, compared to predrug ACSF; n = 7; Fig. 4C) but had no effect on EPSCs ($P > 0.05$, paired t-test, compared to predrug ACSF n = 6; Fig. 4B). IPSCs were not only blocked by bicuculline but also by AP5 and CNQX, consistent with glutamate-driven GABAergic feedforward inhibition (see 2.7.3). Yellow light stimulation (590 nm) served as a control and had no effect. The data suggest that KOR activation inhibits parabrachial glutamatergic input-driven synaptic inhibition of CeA-CRF neurons, but not direct excitatory parabrachial input to these neurons, which is consistent with an inhibitory action on inhibitory neurons that account for synaptic inhibition, resulting in disinhibition of CeA-CRF neurons.

To determine the site of action of U-69,593 on inhibitory transmission we analyzed spontaneous IPSCs (sIPSCs, Fig. 5) and miniature IPSCs (mIPSCs, Fig. 6) in visually identified CeA-CRF neurons (see 2.7.3). Cumulative distribution analysis showed that U-69,593 (1 μM; 15 min) decreased frequency, but not amplitude, of sIPSCs significantly ($P < 0.01$, paired t-test compared to predrug ACSF, $n = 6$; Fig. 5). Similarly, U-69,593 decreased frequency, but not amplitude, of mIPSCs significantly ($P < 0.01$, paired t-test compared to predrug ACSF, $n = 6$; Fig. 6). IPSC kinetics were not affected by U-69,593 (Figs. 5B and 6B). The data suggest that KOR activation causes decreased synaptic inhibition of CeA-CRF neurons (disinhibition).

The consequences of the facilitatory (disinhibitory) effects of U-69,593 on neuronal CeA-CRF network activity were analyzed by measuring synaptically evoked calcium signals in CeA-CRF neurons (see 2.7.4). Calcium transients were evoked in CRF neurons expressing a fluorescent calcium indicator (GCaMP6f) by electrical stimulation (2.0 mA, 0.5 ms) of presumed parabrachial afferents as in previous studies from our group (Fu and Neugebauer, 2008; Neugebauer et al., 2003; Ren et al., 2013; Thompson et al., 2018) and others (Ikeda et al., 2007; Nakao et al., 2012; Watabe et al., 2013) (see 2.7.4 and Discussion). Parabrachial afferents run in a clearly visible fiber tract dorsomedial to the CeA and ventral to but outside of the caudate-putamen area (Sarhan et al., 2005) and can by activated electrically or optogenetically (Ikeda et al., 2007; Neugebauer et al., 2003; Sugimura et al., 2016). Neurons were visualized and signals were recorded with a multiphoton system. Neurons were selected that showed an increase in calcium signals in response to synaptic stimulation (see Fig. 7D). U-69,593 (1 μM, 15 min) increased calcium transients in CeA-CRF neurons significantly ($n = 20$ neurons, 4 rats; $P < 0.001$, paired t-test, compared to predrug control).

4. Discussion

The dynorphin/kappa opioid receptor (KOR) system plays an important role in stress responses and negative affective states through actions in limbic brain areas such as the amygdala (Bruchas et al., 2010; Crowley et al., 2016; Lalanne et al., 2014; Land et al., 2008; Smith et al., 2012; Tejeda et al., 2017). The amygdala is an integrative center for emotional-affective behaviors and related disorders such as anxiety, depression, drug addiction and alcohol use disorders (Apkarian et al., 2013; Koob and Schulkin, 2019; Phelps and Ledoux, 2005); and the amygdala is critically involved in the averse-affective aspects of pain and pain modulation (Neugebauer et al., 2004; Thompson and Neugebauer, 2019). Recent evidence suggests that KOR signaling in the central nucleus of the amygdala (CeA) contributes to the averse-affective behaviors in stress- or injury-induced pain conditions.

Mechanisms of KOR function in the CeA related to pain are only beginning to emerge. The synaptic and cellular actions of KOR activation remain to be determined, and this knowledge gap was addressed here. We focused on CRF neurons in the CeA because they are a major source of dynorphin in the amygdala (Marchant et al., 2007) and project to extra-amygdalar targets to modulate averse-affective behaviors (Beckerman et al., 2013; Fendt et al., 1997; Marcilhac and Siaud, 1997; McCall et al., 2015; Pomrenze et al., 2019; Pomrenze et al., 2015; Reyes et al., 2011); KOR is expressed in the CeA at particularly high levels (Cahill et al., 2014; Le Merrer et al., 2009; Mansour et al., 1996; Mansour et al., 1995), and stress-

related KOR phosphorylation in the amygdala (Bruchas et al., 2009; Xie et al., 2017) has been linked to dynorphin downstream of CRF signaling (Bruchas et al., 2009). We studied KOR and CRF function in the right CeA because evidence from previous studies suggests right-hemispheric lateralization of KOR function (Nation et al., 2018; Navratilova et al., 2020; Phelps et al., 2019) and pain-related signaling (Carrasquillo and Gereau, 2008; Goncalves and Dickenson, 2012; Ji and Neugebauer, 2009) in the CeA. A KOR antagonist administered into the right, but not left, CeA prevented gabapentin-induced conditioned place preference without affecting mechanosensitivity in a neuropathic pain model (Navratilova et al., 2019), suggesting elimination of the aversive qualities of ongoing pain. Blockade of KOR in the right, but not left, CeA also restored descending pain control (diffuse noxious inhibitory control, DNIC) that was lost in stress conditions (Nation et al., 2018) or neuropathic pain (Liu et al., 2019; Phelps et al., 2019).

Here we show that a selective KOR agonist (U-69,593) (Zhou et al., 2013) administered into the CeA or applied systemically in naive animals causes increased emotional responses (ultrasonic vocalizations), anxiety-like behaviors (open field test), and avoidance behaviors. Systemic KOR agonist application has been reported before to produce place aversion in a neuropathic pain model (Liu et al., 2019). Importantly, the effects of systemically applied U-69,593 were blocked by optogenetic silencing of CRF neurons (activation of halorhodopsin with yellow light; see 2.4.1), whereas blue light as an important control had no effect (Fig. 3B and D). For optogenetic stimulation we used parameters that were employed successfully in other studies to activate (Sugimura et al., 2016) or silence (De Guglielmo et al., 2019) CeA neurons. U-69,593 had no effect on nociceptive mechanical thresholds, which is consistent with previous results showing that KOR signaling contributes to averse-affective rather than sensory aspects of pain (Navratilova et al., 2019), and may suggest that the neurocircuitry involved in descending control of spinal reflexes was not engaged by KOR activation of CeA-CRF neurons. As a note of caution, the downstream targets of CRF neurons were not determined in the present study with optogenetic manipulations in the CeA. However, the effects of systemic KOR agonist application could not be explained by the activation of KOR expressed on the terminals of CeA-CRF neurons or on neurons in target regions downstream of CeA-CRF neurons, because activation of inhibitory KOR and optical silencing of CRF neurons would have similar rather than opposing effects as observed here. Synaptic and cellular mechanisms of pain-related KOR function in the amygdala are not well understood, but our previous study found that a KOR antagonist increased synaptic inhibition to decrease synaptically evoked spiking of CeA neurons in brain slices, suggesting feedforward inhibition was compromised in the pain state but could be restored by KOR blockade (Navratilova et al., 2019). The CeA neurons were identified by their firing properties and location in the lateral-capsular CeA, and we suggested that they might be CRF neurons.

In the present study, we recorded visually identified CeA-CRF neurons in brain slices from transgenic rats to test the hypothesis that activation of KOR would inhibit inhibitory synaptic transmission onto these neurons, resulting in disinhibition and increased neuronal activity (see Fig. 4A). The slice physiology experiments show for the first time that a selective KOR agonist decreased inhibitory synaptic transmission onto CeA-CRF neurons (Fig. 4). Synaptic responses were evoked by selective optical (blue light) stimulation of ChR2 expressing

terminals in the CeA originating from glutamatergic parabrachial afferents. Their activation produced a monosynaptic excitatory (EPSC) and glutamate-driven polysynaptic inhibitory (IPSC) response (Fig. 4). Yellow light application as a control did not evoke any synaptic responses. IPSCs were blocked not only with a $GABA_A$ receptor antagonist (bicuculline) but also with glutamate receptor antagonists (AP5 and CNQX), suggesting glutamate-driven feedforward inhibition of CeA-CRF neurons. We did not attempt to block the effects of U-69,593 with a KOR antagonist but it was shown previously that nor-BNI antagonized the effects of U-69,593 on inhibitory synaptic transmission in the CeA (Kang-Park et al., 2013).

The KOR agonist acted presynaptically on terminals of inhibitory interneurons, because analysis of spontaneous and miniature IPSCs showed that U-69,593 decreased frequency but not amplitude of sIPSCs and mIPSCs (Figs. 5 and 6). While changes in frequency of sIPSCs can involve a network action, changes in frequency of mIPSCs (in TTX) point to an action-potential independent mechanism of presynaptic inhibition of synaptic inhibition (disinhibition). This line of analysis is a well-established electrophysiological approach to determine pre- or postsynaptic mechanisms (for recent studies from our group see Neugebauer (Kiritoshi and Neugebauer, 2015; Kiritoshi et al., 2013; Ren et al., 2013)). The presence of sIPSCs in CRF neurons suggest a tonic inhibitory tone in the absence of synaptic stimulation, which could explain effects of KOR activation on non-evoked behaviors in the open field and place preference tests. Inhibitory interneurons that were inhibited by KOR activation and thus contributed to KOR-mediated feedforward inhibition of CeA-CRF neurons could include PKCdelta, somatostatin or other interneurons in the CeA or intercalated cells. Dynorphin or U-69–593 also decreased inhibitory GABAergic synaptic transmission in CeM neurons (Gilpin et al., 2014; Kang-Park et al., 2013, 2015), but these neurons are not the direct target of parabrachial input, which is an important source of nociceptive information to the amygdala. U-69,593 had no effect on excitatory transmission of parabrachial input to unidentified neurons in the laterocapsular CeA in a previous study (Kissiwaa et al., 2020), which is what we found here with CRF neurons, suggesting that KOR does not modulate excitatory parabrachial input to CeA. Effects on inhibitory synaptic transmission were not explored in that previous study. We interpret our data to suggest that KOR activation inhibits inhibitory interneurons that are activated by glutamatergic input from the parabrachial nucleus and project to CeA-CRF neurons (Fig. 4A), resulting in impaired feedforward inhibition hence KOR-mediated disinhibition of CeA-CRF neurons.

Calcium imaging experiments showed that KOR activation increased activity in CeA-CRF neurons, which would be expected to translate into increased output from these neurons. As mentioned before, CeA-CRF neurons form widespread connections to various extra-amygdalar targets. Our behavioral experiments suggest that CeA-CRF neuronal activation contributes critically to the facilitatory behavioral effects of KOR activation, because silencing of CRF neurons in the CeA blocked the effects of the KOR agonist (Fig. 3). The downstream consequences of CeA-CRF activation and output remain to be determined.

As a note of caution, in the calcium imaging experiments we did not use optogenetic activation of parabrachial input but stimulated presumed parabrachial afferents by positioning the stimulation electrode under microscopic control on the clearly visible fiber tract that runs dorsomedial to the CeA and ventral to but outside of the caudate-putamen

area as described before by our group (Fu and Neugebauer, 2008; Neugebauer et al., 2003; Ren et al., 2013; Thompson et al., 2018) and others (Ikeda et al., 2007; Nakao et al., 2012; Watabe et al., 2013). This fiber tract has been reconstructed anatomically and described in great detail (Sarhan et al., 2005), and no afferents to the CeA other than from parabrachial area have been described in this area (Harrigan et al., 1994; Schwaber et al., 1988), but we cannot exclude the possibility that fibers from other sources were activated in this set of experiments. However, the effects of U-69,593 on calcium signals of CeA-CRF neurons matched the decrease of feedforward inhibition of these neuron (disinhibition) evoked by optogenetic stimulation of parabrachial afferent terminals.

Microdialysis drug application also deserves consideration. Steady state drug application without volume effect are advantages of this technique, but the exact drug concentration in the tissue can only be estimated. The concentration of U-69,593 (100 μM) in the microdialysis probe was about 100 fold higher than the intended target concentration based on information in the literature (Zhou et al., 2013) because of the concentration gradient across the microdialysis membrane. The 100 fold factor is supported by our previous studies comparing drug effects in brain slices with microdialysis drug application for several drugs (Fu and Neugebauer, 2008; Kiritoshi et al., 2016; Li et al., 2011; Ren et al., 2013; Thompson et al., 2018). Importantly, microdialysis application of U-69,593 (100 μM) in the behavioral experiments produced similar facilitatory effects as superfusion of U-69,593 (1 μM) onto the brain slice in our ex vivo electrophysiology studies, providing further support of the selection of drug concentrations.

5. Conclusions

This study shows for the first time that KOR activation in the amygdala facilitates averse-affective rather than sensory pain-like behaviors through a mechanism that involves synaptic disinhibition of CRF neurons. KOR activation presynaptically inhibited synaptic inhibition (disinhibition) that was driven by glutamatergic parabrachial input to the CeA (feedforward inhibition). These effects were observed in naïve animals and disinhibition of CRF neurons could therefore be a mechanism of so-called functional pain conditions that are characterized by the absence of tissue injury or pathology. Blockade of KOR signaling in the right CeA could have potential therapeutic implications.

Acknowledgements

This work was supported by NIH grants NS038261 (VN), NS106902 (VN and FP), DA041809 (FP), and NS109255 (GJ and EN). We thank Dr. Robert Messing, University of Texas at Austin, for kindly providing the initial Crh-Cre rat breeding pairs.

References

Allen HN, Bobnar HJ, Kolber BJ, 2020 Left and right hemispheric lateralization of the amygdala in pain. Prog Neurobiol, 101891. [PubMed: 32730859]

Apkarian AV, Neugebauer V, Koob G, Edwards S, Levine JD, Ferrari L, Egli M, Regunathan S, 2013 Neural mechanisms of pain and alcohol dependence. Pharmacol. Biochem. Behav 112C, 34–41.

Beckerman MA, Van Kempen TA, Justice NJ, Milner TA, Glass MJ, 2013 Corticotropin-releasing factor in the mouse central nucleus of the amygdala: ultrastructural distribution in NMDA-NR1

receptor subunit expressing neurons as well as projection neurons to the bed nucleus of the stria terminalis. Exp. Neurol 239, 120–132. [PubMed: 23063907]

Bruchas MR, Land BB, Chavkin C, 2010 The dynorphin/kappa opioid system as a modulator of stress-induced and pro-addictive behaviors. Brain Res 1314, 44–55. [PubMed: 19716811]

Bruchas MR, Land BB, Lemos JC, Chavkin C, 2009 CRF1-R activation of the dynorphin/kappa opioid system in the mouse basolateral amygdala mediates anxiety-like behavior. PLoS. One 4, e8528. [PubMed: 20052275]

Cahill CM, Taylor AM, Cook C, Ong E, Moron JA, Evans CJ, 2014 Does the kappa opioid receptor system contribute to pain aversion? Front Pharmacol 5, 253. [PubMed: 25452729]

Carrasquillo Y, Gereau RW, 2008 Hemispheric lateralization of a molecular signal for pain modulation in the amygdala. Mol. Pain 4, 24. [PubMed: 18573207]

Chieng BC, Christie MJ, Osborne PB, 2006 Characterization of neurons in the rat central nucleus of the amygdala: cellular physiology, morphology, and opioid sensitivity. J Comp Neurol 497, 910–927. [PubMed: 16802333]

Corder G, Ahanonu B, Grewe BF, Wang D, Schnitzer MJ, Scherrer G, 2019 An amygdalar neural ensemble that encodes the unpleasantness of pain. Science 363, 276–281. [PubMed: 30655440]

Crowley NA, Bloodgood DW, Hardaway JA, Kendra AM, McCall JG, Al-Hasani R, McCall NM, Yu W, Schools ZL, Krashes MJ, Lowell BB, Whistler JL, Bruchas MR, Kash TL, 2016 Dynorphin Controls the Gain of an Amygdalar Anxiety Circuit. Cell Rep 14, 2774–2783. [PubMed: 26997280]

De Guglielmo G, Kallupi M, Pomrenze MB, Crawford E, Simpson S, Schweitzer P, Koob GF, Messing RO, George O, 2019 Inactivation of a CRF-dependent amygdalofugal pathway reverses addiction-like behaviors in alcohol-dependent rats. Nat. Commun 10, 1238. [PubMed: 30886240]

Fendt M, Koch M, Schnitzler HU, 1997 Corticotropin-releasing factor in the caudal pontine reticular nucleus mediates the expression of fear-potentiated startle in the rat. Eur. J. Neurosci 9, 299–305. [PubMed: 9058050]

Fu Y, Han J, Ishola T, Scerbo M, Adwanikar H, Ramsey C, Neugebauer V, 2008 PKA and ERK, but not PKC, in the amygdala contribute to pain-related synaptic plasticity and behavior. Mol. Pain 4, 26–46. [PubMed: 18631385]

Fu Y, Neugebauer V, 2008 Differential mechanisms of CRF1 and CRF2 receptor functions in the amygdala in pain-related synaptic facilitation and behavior. J Neurosci 28, 3861–3876. [PubMed: 18400885]

Gilpin NW, Roberto M, Koob GF, Schweitzer P, 2014 Kappa opioid receptor activation decreases inhibitory transmission and antagonizes alcohol effects in rat central amygdala. Neuropharmacology 77, 294–302. [PubMed: 24157490]

Goncalves L, Dickenson AH, 2012 Asymmetric time-dependent activation of right central amygdala neurones in rats with peripheral neuropathy and pregabalin modulation. Eur. J. Neurosci 36, 3204–3213. [PubMed: 22861166]

Han JS, Bird GC, Li W, Neugebauer V, 2005 Computerized analysis of audible and ultrasonic vocalizations of rats as a standardized measure of pain-related behavior. J. Neurosci. Meth 141, 261–269.

Harrigan EA, Magnuson DJ, Thunstedt GM, Gray TS, 1994 Corticotropin releasing factor neurons are innervated by calcitonin gene-related peptide terminals in the rat central amygdaloid nucleus. Brain Res. Bull 33, 529–534. [PubMed: 8186998]

Ikeda R, Takahashi Y, Inoue K, Kato F, 2007 NMDA receptor-independent synaptic plasticity in the central amygdala in the rat model of neuropathic pain. Pain 127, 161–172. [PubMed: 17055162]

Ji G, Li Z, Neugebauer V, 2015 Reactive oxygen species mediate visceral pain-related amygdala plasticity and behaviors. Pain 156, 825–836. [PubMed: 25734993]

Ji G, Neugebauer V, 2009 Hemispheric lateralization of pain processing by amygdala neurons. J Neurophysiol 1102, 2253–2264.

Ji G, Yakhnitsa V, Kiritoshi T, Presto P, Neugebauer V, 2018 Fear extinction learning ability predicts neuropathic pain behaviors and amygdala activity in male rats. Mol. Pain 14, 1744806918804441. [PubMed: 30209982]

Kang-Park M, Kieffer BL, Roberts AJ, Siggins GR, Moore SD, 2013 kappa-Opioid receptors in the central amygdala regulate ethanol actions at presynaptic GABAergic sites. J. Pharmacol. Exp. Ther 346, 130–137. [PubMed: 23587526]

Kang-Park M, Kieffer BL, Roberts AJ, Siggins GR, Moore SD, 2015 Interaction of CRF and kappa opioid systems on GABAergic neurotransmission in the mouse central amygdala. J. Pharmacol. Exp. Ther 355, 206–211. [PubMed: 26350161]

Kim H, Thompson J, Ji G, Ganapathy V, Neugebauer V, 2017 Monomethyl fumarate inhibits pain behaviors and amygdala activity in a rat arthritis model. Pain 158, 2376–2385. [PubMed: 28832396]

King T, Vera-Portocarrero L, Gutierrez T, Vanderah TW, Dussor G, Lai J, Fields HL, Porreca F, 2009 Unmasking the tonic-aversive state in neuropathic pain. Nat. Neurosci 12, 1364–1366. [PubMed: 19783992]

Kiritoshi T, Ji G, Neugebauer V, 2016 Rescue of Impaired mGluR5-Driven Endocannabinoid Signaling Restores Prefrontal Cortical Output to Inhibit Pain in Arthritic Rats. J. Neurosci 36, 837–850. [PubMed: 26791214]

Kiritoshi T, Neugebauer V, 2015 Group II mGluRs modulate baseline and arthritis pain-related synaptic transmission in the rat medial prefrontal cortex. Neuropharmacology 95, 388–394. [PubMed: 25912637]

Kiritoshi T, Neugebauer V, 2018 Pathway-Specific Alterations of Cortico-Amygdala Transmission in an Arthritis Pain Model. ACS Chem. Neurosci 9, 2252–2261. [PubMed: 29630339]

Kiritoshi T, Sun H, Ren W, Stauffer SR, Lindsley CW, Conn PJ, Neugebauer V, 2013 Modulation of pyramidal cell output in the medial prefrontal cortex by mGluR5 interacting with CB1. Neuropharmacology 66, 170–178. [PubMed: 22521499]

Kissiwaa SA, Patel SD, Winters BL, Bagley EE, 2020 Opioids differentially modulate two synapses important for pain processing in the amygdala. Br J Pharmacol 177, 420–431. [PubMed: 31596498]

Kolber BJ, Montana MC, Carrasquillo Y, Xu J, Heinemann SF, Muglia LJ, Gereau RW, 2010 Activation of metabotropic glutamate receptor 5 in the amygdala modulates pain-like behavior. J. Neurosci 30, 8203–8213. [PubMed: 20554871]

Koob GF, Schulkin J, 2019 Addiction and stress: An allostatic view. Neurosci Biobehav. Rev 106, 245–262. [PubMed: 30227143]

Lalanne L, Ayranci G, Kieffer BL, Lutz PE, 2014 The kappa opioid receptor: from addiction to depression, and back. Front Psychiatry 5, 170. [PubMed: 25538632]

Land BB, Bruchas MR, Lemos JC, Xu M, Melief EJ, Chavkin C, 2008 The dysphoric component of stress is encoded by activation of the dynorphin kappa-opioid system. J. Neurosci 28, 407–414. [PubMed: 18184783]

Le Merrer J, Becker JA, Befort K, Kieffer BL, 2009 Reward processing by the opioid system in the brain. Physiol Rev 89, 1379–1412. [PubMed: 19789384]

Li Z, Ji G, Neugebauer V, 2011 Mitochondrial reactive oxygen species are activated by mGluR5 through IP3 and activate ERK and PKA to increase excitability of amygdala neurons and pain behavior. J. Neurosci 31, 1114–1127. [PubMed: 21248136]

Liu SS, Pickens S, Burma NE, Ibarra-Lecue I, Yang H, Xue L, Cook C, Hakimian JK, Severino AL, Lueptow L, Komarek K, Taylor AMW, Olmstead MC, Carroll FI, Bass CE, Andrews AM, Walwyn W, Trang T, Evans CJ, Leslie FM, Cahill CM, 2019 Kappa Opioid Receptors Drive a Tonic Aversive Component of Chronic Pain. J. Neurosci 39, 4162–4178. [PubMed: 30862664]

Mansour A, Burke S, Pavlic RJ, Akil H, Watson SJ, 1996 Immunohistochemical localization of the cloned kappa 1 receptor in the rat CNS and pituitary. Neuroscience 71, 671–690. [PubMed: 8867040]

Mansour A, Fox CA, Akil H, Watson SJ, 1995 Opioid-receptor mRNA expression in the rat CNS: anatomical and functional implications. TINS 18, 22–29. [PubMed: 7535487]

Marchant NJ, Densmore VS, Osborne PB, 2007 Coexpression of prodynorphin and corticotrophin-releasing hormone in the rat central amygdala: evidence of two distinct endogenous opioid systems in the lateral division. J. Comp Neurol 504, 702–715. [PubMed: 17722034]

Marcilhac A, Siaud P, 1997 Identification of projections from the central nucleus of the amygdala to the paraventricular nucleus of the hypothalamus which are immunoreactive for corticotrophin-releasing hormone in the rat. Exp. Physiol 82, 273–281. [PubMed: 9129941]

Mazzitelli M, Neugebauer V, 2019 Amygdala group II mGluRs mediate the inhibitory effects of systemic group II mGluR activation on behavior and spinal neurons in a rat model of arthritis pain. Neuropharmacology 158, 107706. [PubMed: 31306647]

McCall JG, Al-Hasani R, Siuda ER, Hong DY, Norris AJ, Ford CP, Bruchas MR, 2015 CRH Engagement of the Locus Coeruleus Noradrenergic System Mediates Stress-Induced Anxiety. Neuron 87, 605–620. [PubMed: 26212712]

Nakao A, Takahashi Y, Nagase M, Ikeda R, Kato F, 2012 Role of capsaicin-sensitive C-fiber afferents in neuropathic pain-induced synaptic potentiation in the nociceptive amygdala. Mol. Pain 8, 51. [PubMed: 22776418]

Nation KM, De FM, Hernandez PI, Dodick DW, Neugebauer V, Navratilova E, Porreca F, 2018 Lateralized kappa opioid receptor signaling from the amygdala central nucleus promotes stress-induced functional pain. Pain 159, 919–928. [PubMed: 29369967]

Navratilova E, Ji G, Phelps C, Qu C, Hein M, Yakhnitsa V, Neugebauer V, Porreca F, 2019 Kappa opioid signaling in the central nucleus of the amygdala promotes disinhibition and aversiveness of chronic neuropathic pain. Pain 160, 824–832. [PubMed: 30681985]

Navratilova E, Nation K, Remeniuk B, Neugebauer V, Bannister K, Dickenson AH, Porreca F, 2020 Selective modulation of tonic aversive qualities of neuropathic pain by morphine in the central nucleus of the amygdala requires endogenous opioid signaling in the anterior cingulate cortex. Pain 161, 609–618. [PubMed: 31725062]

Neugebauer V, 2020 Amygdala Physiology in Pain. Handbook of Behavioral Neurosciences 26, 101–113.

Neugebauer V, Han JS, Adwanikar H, Fu Y, Ji G, 2007 Techniques for assessing knee joint pain in arthritis. Mol. Pain 3, 8–20. [PubMed: 17391515]

Neugebauer V, Li W, Bird GC, Bhave G, Gereau RW, 2003 Synaptic plasticity in the amygdala in a model of arthritic pain: differential roles of metabotropic glutamate receptors 1 and 5. J. Neurosci 23, 52–63. [PubMed: 12514201]

Neugebauer V, Li W, Bird GC, Han JS, 2004 The amygdala and persistent pain. Neuroscientist 10, 221–234. [PubMed: 15155061]

Paxinos G, Watson C, 1998 The rat brain in stereotaxic coordinates. Academic Press, New York.

Phelps CE, Navratilova E, Dickenson AH, Porreca F, Bannister K, 2019 Kappa opioid signaling in the right central amygdala causes hind paw specific loss of diffuse noxious inhibitory controls in experimental neuropathic pain. Pain 160, 1614–1621. [PubMed: 30870321]

Phelps EA, Ledoux JE, 2005 Contributions of the Amygdala to Emotion Processing: From Animal Models to Human Behavior. Neuron 48, 175–187. [PubMed: 16242399]

Pomrenze MB, Giovanetti SM, Maiya R, Gordon AG, Kreeger LJ, Messing RO, 2019 Dissecting the Roles of GABA and Neuropeptides from Rat Central Amygdala CRF Neurons in Anxiety and Fear Learning. Cell Rep 29, 13–21. [PubMed: 31577943]

Pomrenze MB, Millan EZ, Hopf FW, Keiflin R, Maiya R, Blasio A, Dadgar J, Kharazia V, De GG, Crawford E, Janak PH, George O, Rice KC, Messing RO, 2015 A Transgenic Rat for Investigating the Anatomy and Function of Corticotrophin Releasing Factor Circuits. Front Neurosci 9, 487. [PubMed: 26733798]

Ren W, Kiritoshi T, Gregoire S, Ji G, Guerrini R, Calo G, Neugebauer V, 2013 Neuropeptide S: a novel regulator of pain-related amygdala plasticity and behaviors. J. Neurophysiol 110, 1765–1781. [PubMed: 23883857]

Reyes BA, Carvalho AF, Vakharia K, van Bockstaele EJ, 2011 Amygdalar peptidergic circuits regulating noradrenergic locus coeruleus neurons: linking limbic and arousal centers. Exp. Neurol 230, 96–105. [PubMed: 21515261]

Sarhan M, Freund-Mercier MJ, Veinante P, 2005 Branching patterns of parabrachial neurons projecting to the central extended amgydala: single axonal reconstructions. J Comp Neurol 491, 418–442. [PubMed: 16175547]

Schwaber JS, Sternini C, Brecha NC, Rogers WT, Card JP, 1988 Neurons containing calcitonin gene-related peptide in the parabrachial nucleus project to the central nucleus of the amygdala. J. Comp. Neurol 270, 416–426. [PubMed: 2836477]

Smith JS, Schindler AG, Martinelli E, Gustin RM, Bruchas MR, Chavkin C, 2012 Stress-induced activation of the dynorphin/kappa-opioid receptor system in the amygdala potentiates nicotine conditioned place preference. J. Neurosci 32, 1488–1495. [PubMed: 22279233]

Standifer KM, Pasternak GW, 1997 G proteins and opioid receptor-mediated signalling. Cell Signal 9, 237–248. [PubMed: 9218123]

Sugimura YK, Takahashi Y, Watabe AM, Kato F, 2016 Synaptic and network consequences of monosynaptic nociceptive inputs of parabrachial nucleus origin in the central amygdala. J. Neurophysiol, 2721–2739. [PubMed: 26888105]

Tejeda HA, Wu J, Kornspun AR, Pignatelli M, Kashtelyan V, Krashes MJ, Lowell BB, Carlezon WA Jr., Bonci A, 2017 Pathway- and Cell-Specific Kappa-Opioid Receptor Modulation of Excitation-Inhibition Balance Differentially Gates D1 and D2 Accumbens Neuron Activity. Neuron 93, 147–163. [PubMed: 28056342]

Thompson JM, Ji G, Neugebauer V, 2015 Small-conductance calcium-activated potassium (SK) channels in the amygdala mediate pain-inhibiting effects of clinically available riluzole in a rat model of arthritis pain. Mol. Pain 11, 51. [PubMed: 26311432]

Thompson JM, Neugebauer V, 2019 Cortico-limbic pain mechanisms. Neurosci. Lett 702, 15–23. [PubMed: 30503916]

Thompson JM, Yakhnitsa V, Ji G, Neugebauer V, 2018 Small conductance calcium activated potassium (SK) channel dependent and independent effects of riluzole on neuropathic pain-related amygdala activity and behaviors in rats. Neuropharmacology 138, 219–231. [PubMed: 29908238]

Watabe AM, Ochiai T, Nagase M, Takahashi Y, Sato M, Kato F, 2013 Synaptic potentiation in the nociceptive amygdala following fear learning in mice. Mol. Brain 6, 11. [PubMed: 23452928]

Wilson TD, Valdivia S, Khan A, Ahn HS, Adke AP, Martinez GS, Sugimura YK, Carrasquillo Y, 2019 Dual and Opposing Functions of the Central Amygdala in the Modulation of Pain. Cell Rep 29, 332–346. [PubMed: 31597095]

Xie JY, De FM, Kopruszinski CM, Eyde N, LaVigne J, Remeniuk B, Hernandez P, Yue X, Goshima N, Ossipov M, King T, Streicher JM, Navratilova E, Dodick D, Rosen H, Roberts E, Porreca F, 2017 Kappa opioid receptor antagonists: A possible new class of therapeutics for migraine prevention. Cephalalgia 37, 780–794. [PubMed: 28376659]

Zhou L, Lovell KM, Frankowski KJ, Slauson SR, Phillips AM, Streicher JM, Stahl E, Schmid CL, Hodder P, Madoux F, Cameron MD, Prisinzano TE, Aube J, Bohn LM, 2013 Development of functionally selective, small molecule agonists at kappa opioid receptors. J. Biol. Chem 288, 36703–36716. [PubMed: 24187130]

Zhu W, Pan ZZ, 2004 Synaptic properties and postsynaptic opioid effects in rat central amygdala neurons. Neuroscience 127, 871–879. [PubMed: 15312899]

Highlights

- Kappa opioid receptors in the amygdala facilitate averse-affective pain behaviors.
- Optogenetic silencing of CRF neurons in the amygdala blocks behavioral effects.
- Kappa opioid receptors attenuate feedforward inhibition of CRF amygdala neurons.
- Kappa opioid receptors act presynaptically to disinhibit CRF neurons.
- Blockade of KOR signaling in the amygdala may have therapeutic implications.

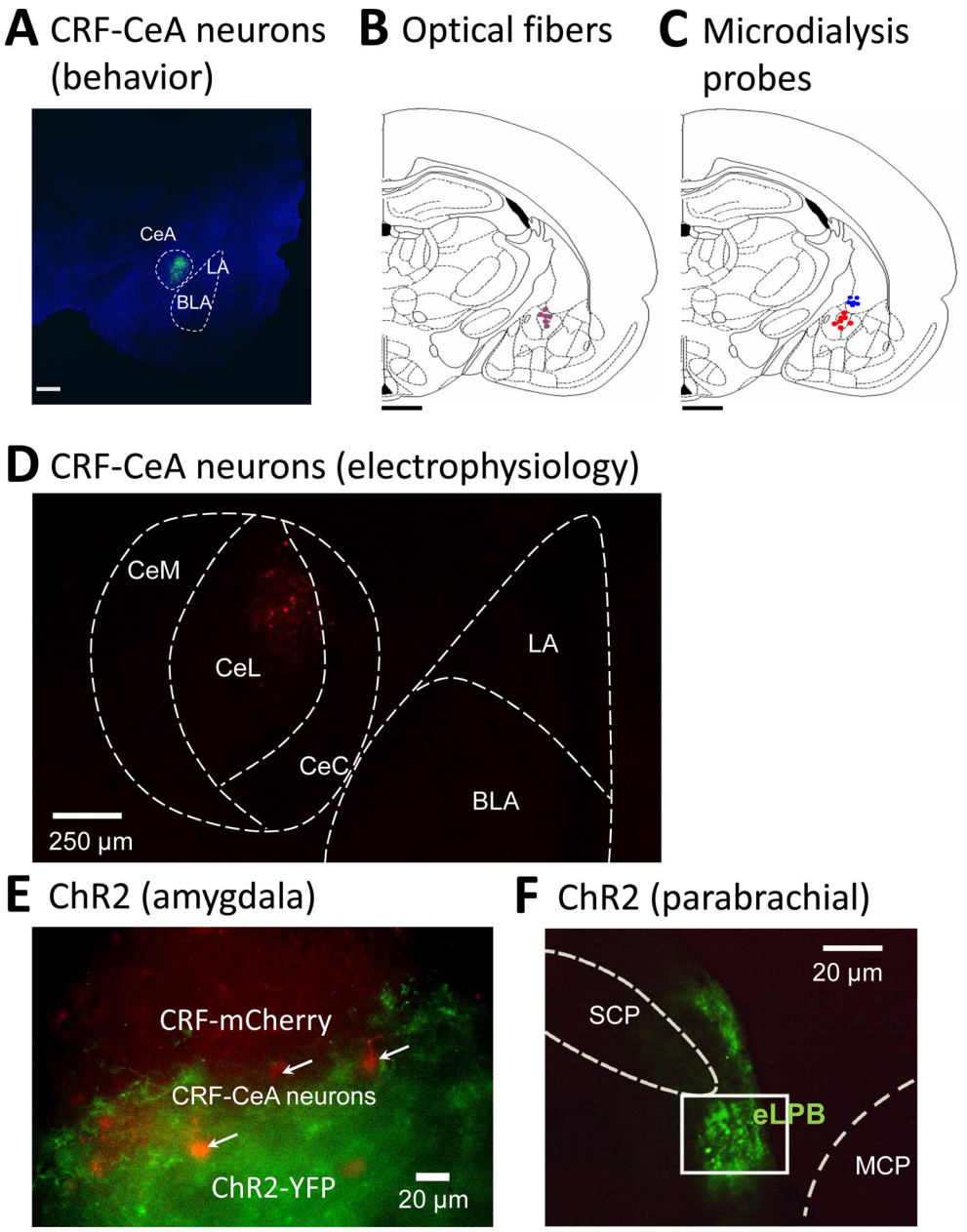

Figure 1. Location of CRF neurons, optical fibers and microdialysis probes in the central nucleus of the amygdala (CeA).

(A) Confocal image of eGFP fluorescence in a brain slice from a Crh-Cre rat shows neurons expressing CRF in the CeA 4–5 weeks after rAAV5/EF1a-DIO-eNpHR3.0-eYFP injection into the CeA. Scale bar, 500 µm. LA, BLA, lateral and basolateral amygdala **(B, C)** Diagrams show coronal brain slices, −2.56 caudal to bregma. Symbols indicate the positions of the tips of optical fibers for yellow light stimulation to silence neurons (B) and of microdialysis fibers for drug application into CeA (red symbols) or striatum (blue symbols; C) in the right CeA. Scale bar, 500mm. **(D)** Confocal image of CRF neurons in the CeA in a brain slice from a Crh-Cre rat 4 weeks after injection of AAV5-EF1α-DIO-mCherry into the CeA. CeC, CeL, CeM, capsular, lateral and medial division of CeA. **(E)** Channelrhodopsin 2

(ChR2) in afferent terminals of glutamatergic neurons of the parabrachial nucleus were visualized in the CeA 4 weeks after injection of rAAV5-CaMKIIa-hChR2(H134R)-eYFP into the parabrachial nucleus (see 1F). CeA-CRF neurons (examples indicated by arrows) are visualized by their expression of mCherry (see D). **(F)** Injection site for rAAV5-CaMKIIa-hChR2(H134R)-eYFP in the external lateral parabrachial area (eLPB) to express ChR2 in glutamatergic neurons. SPC and MCP, superior and middle cerebellar peduncles.

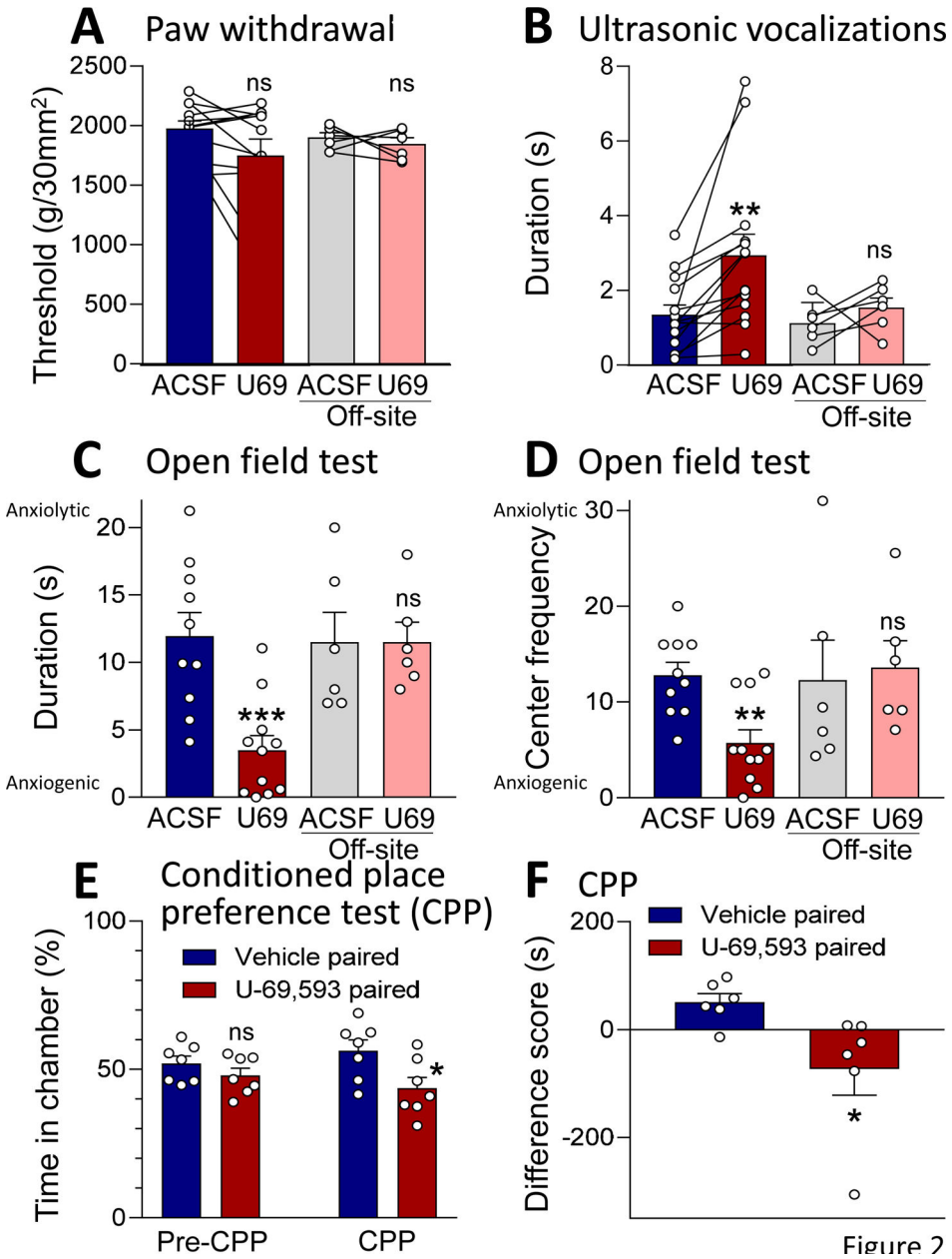

Figure 2. Behavioral effects of a KOR agonist (U-69,593) administered into CeA.

(A) U-69,593 (100 μM in microdialysis probe) administered into the CeA had no significant effect on mechanical withdrawal thresholds. P > 0.05, paired t-test, compared to predrug ACSF control; n = 12. Offsite control administration of U-69,593 into striatum also had no significant effect. P > 0.05, paired t-test compared to ACSF; n = 6. **(B)** U-69,593 increased ultrasonic vocalizations evoked by noxious compression of the knee. ** P < 0.01, paired t-test, compared to predrug ACSF control, n = 14. Offsite control administration of U-69,593 had no effect. P > 0.05, paired t-test compared to ACSF; n = 6. **(C, D)** U-69,593 increased anxiety-like behaviors measured as decreased duration in the center (C) and frequency of entries into the center (D) in the open field test. **,*** P< 0.01, 0.001, t-tests, compared to ACSF control, n = 10 (ACSF), n = 11 (U-69,593). (A-D) Offsite control administration of

U-69,593 had no significant effect $P > 0.05$, paired t-test compared to ACSF; n = 6. **(E, F)** U-69,593 administration caused avoidance of the drug paired chamber in the conditioned place preference test (CPP). (E) Significantly decreased ratio of time spent in drug paired chamber compared to vehicle paired chamber after conditioning (CPP) but not before pairing (pre-CPP). $P < 0.05$, ANOVA with Bonferroni posthoc tests, n = 7. (F) Difference score (time spent in drug or vehicle paired chamber on test day minus time on preconditioning day) was significantly lower for U-69,593 compared to vehicle. $P < 0.05$, t-test, n = 7. Bar histograms show mean ± SEM. Symbols show data from individual animals.

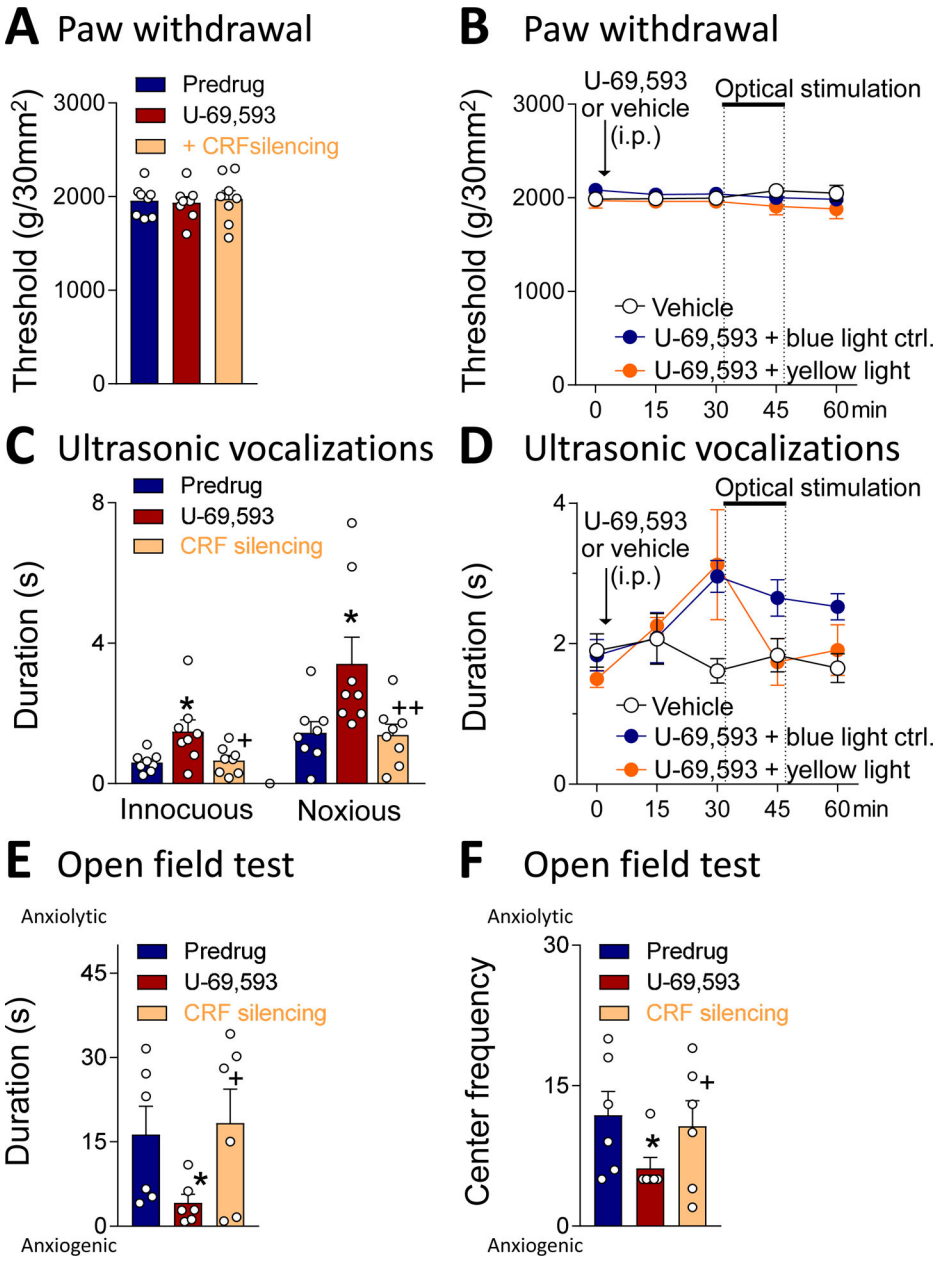

Figure 3. Behavioral effects of systemic application of a KOR agonist (U-69,593) with optical silencing of CeA-CRF neurons.

(A) Compared to predrug, U-69,593 (1.0 mg/kg, intraperitoneally, i.p.) had no effect on mechanical withdrawal thresholds and optical silencing of CeA-CRF neurons (yellow light activation of halorhodopsin; see Materials and Methods) also had no effect (n = 8). **(B)** Time course analysis shows the lack of effect of U-69,593 (1.0 mg/kg, i.p.) in controls (blue light or no light; n = 6) and with optical silencing of CeA-CRF neurons with yellow light (n = 5) compared to vehicle (saline, i.p.) control (n = 6). **(C)** Optogenetic silencing of CeA-CRF neurons reversed the facilitatory effects of systemically applied U-69,593 on ultrasonic vocalizations evoked by noxious compression of the knee (n = 8). **(D)** Time course analysis shows that optical silencing of CeA-CRF neurons with yellow light (n = 5) but not control

interventions (blue light or no light; n = 6) inhibited the effect of U-69,593 (1.0 mg/kg, i.p.) on ultrasonic vocalizations. Vehicle had no effect (n = 6). **(E, F)** Optogenetic silencing of CeA-CRF neurons reversed the anxiogenic-like effects of systemically applied U-69,593 in the open-field test (C, duration in center; D, entries into center; n = 6). Behavioral testing was done 30 min after injection of U-69,953; optical silencing started 15 min later and was done for 15 min followed by behavioral testing at the 60 min time point. * $P < 0.05$, compared to pre-drug (ACSF); $^{+}$ $P < 0.05$, compared to U-69,593 alone; repeated measures ANOVA with Bonferroni posthoc tests. Bar histograms show mean ± SEM. Symbols show data from individual animals.

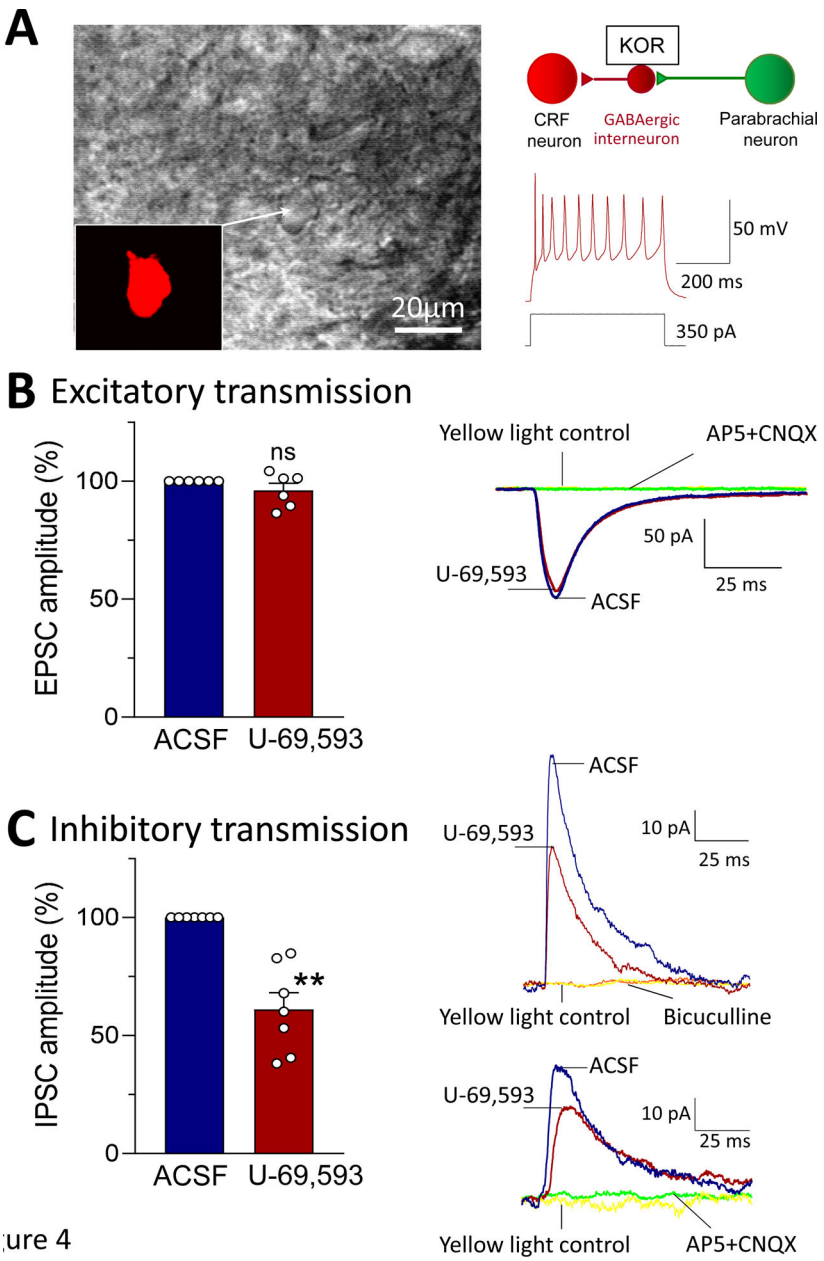

ure 4

Figure 4. Effects of a KOR agonist (U-69,593) on excitatory and inhibitory synaptic transmission in CeA-CRF neurons.

Whole-cell patch-clamp recordings were obtained from visually identified CeA-CRF neurons (see Materials and Methods). **(A)** Hypothesized synaptic circuitry. Individual CeA-CRF neuron is shown in brightfield and with fluorescence (for mCherry) illumination as seen under the microscope. Action potentials were evoked in this regular spiking neuron by intracellular injection of a depolarizing current. **(B)** Excitatory postsynaptic currents (EPSCs) evoked by optical stimulation (472 nm, 10 ms, 12 mW) of ChR2 expressing glutamatergic parabrachial afferents (see Materials and Methods) were not affected by administration of U-69,593 (1 μM) ($n = 6$; $P > 0.05$, paired t-test, compared to predrug ACSF). Traces show an individual example. EPSCs were blocked by AP5 and CNQX (see

2.7.3.). Yellow light (590 nm) stimulation served as a control. **(C)** Inhibitory postsynaptic currents (IPSCs) evoked by optical stimulation of glutamatergic parabrachial afferents were significantly decreased (dis-inhibition) by administration of U-69,593 (n = 7; ** $P < 0.001$, paired t-test, compared to predrug ACSF). Traces show individual examples. IPSCs were blocked by bicuculline (upper example) and by AP5 and CNQX (lower example; see Materials and Methods). Yellow light stimulation served as a control. EPSCs and IPSCs were recorded at −70 mV and 0 mV, respectively. Bar histograms show means ± SEM. Symbols show values of individual neurons.

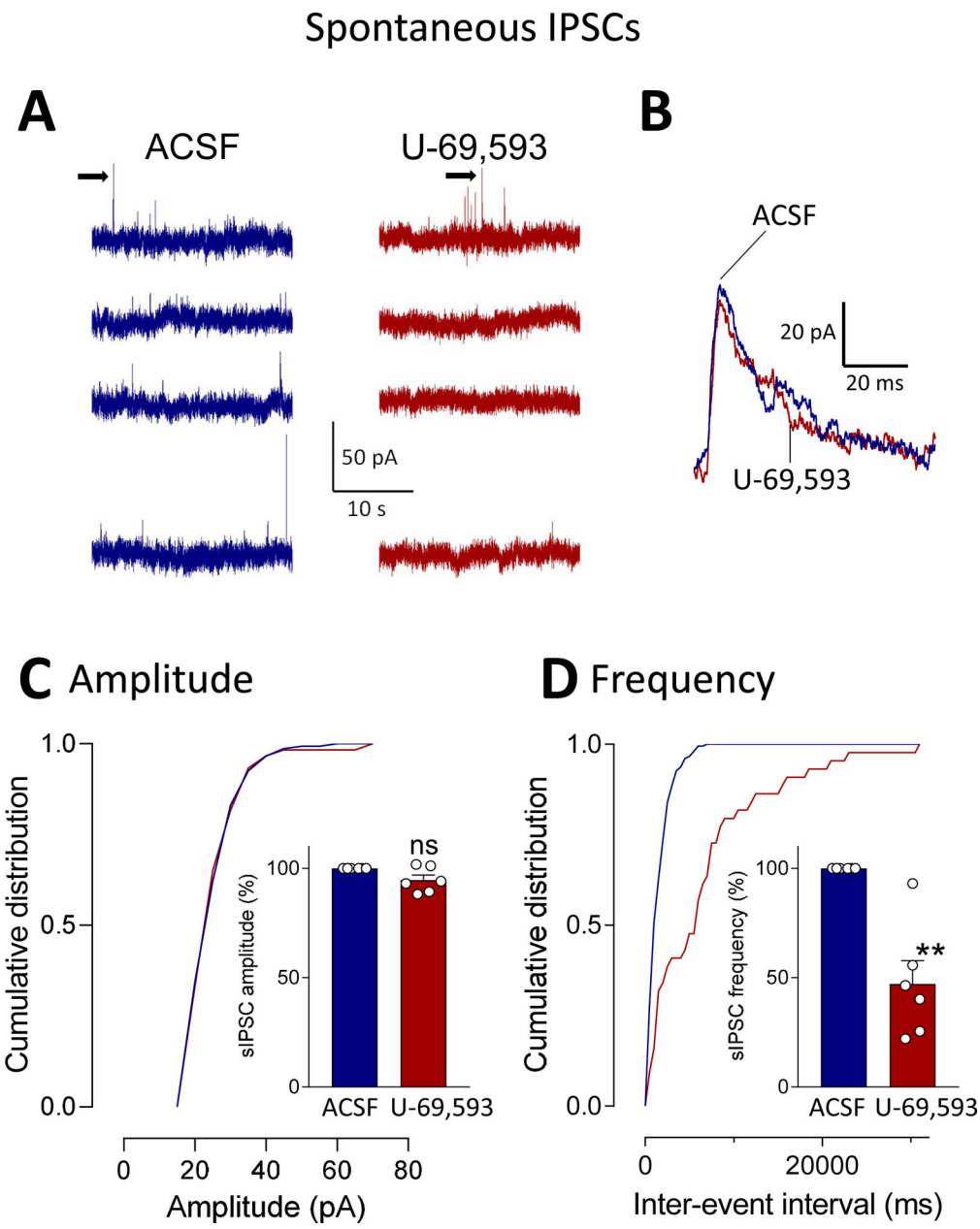

Figure 5. Effects of a KOR agonist (U-69,593) on spontaneous IPSCs (sIPSCs) in CeA-CRF neurons.

Whole-cell patch-clamp recordings were obtained from visually identified CeA-CRF neurons (see Materials and Methods). **(A)** Traces show individual examples of voltage-clamp recordings of sIPSCs during application of vehicle (ACSF) and U-69,593 (1 μM, 15 min). **(B)** Traces of individual sIPSCs (taken from traces in A as indicated by arrows) show that $GABA_A$ channel kinetics were not altered by U-69,593. **(C)** Analysis of cumulative distribution (individual neuron) and mean sIPSC amplitude showed that U-69,593 had no significant effect on amplitude ($n = 6$; $P > 0.05$, paired t-test, compared to ACSF predrug control). **(D)** U-69,593 decreased sIPSC frequency significantly ($n = 6$; $P < 0.01$, paired t-

test compared to predrug ACSF). Bar histograms show means ± SEM. Symbols show values of individual neurons.

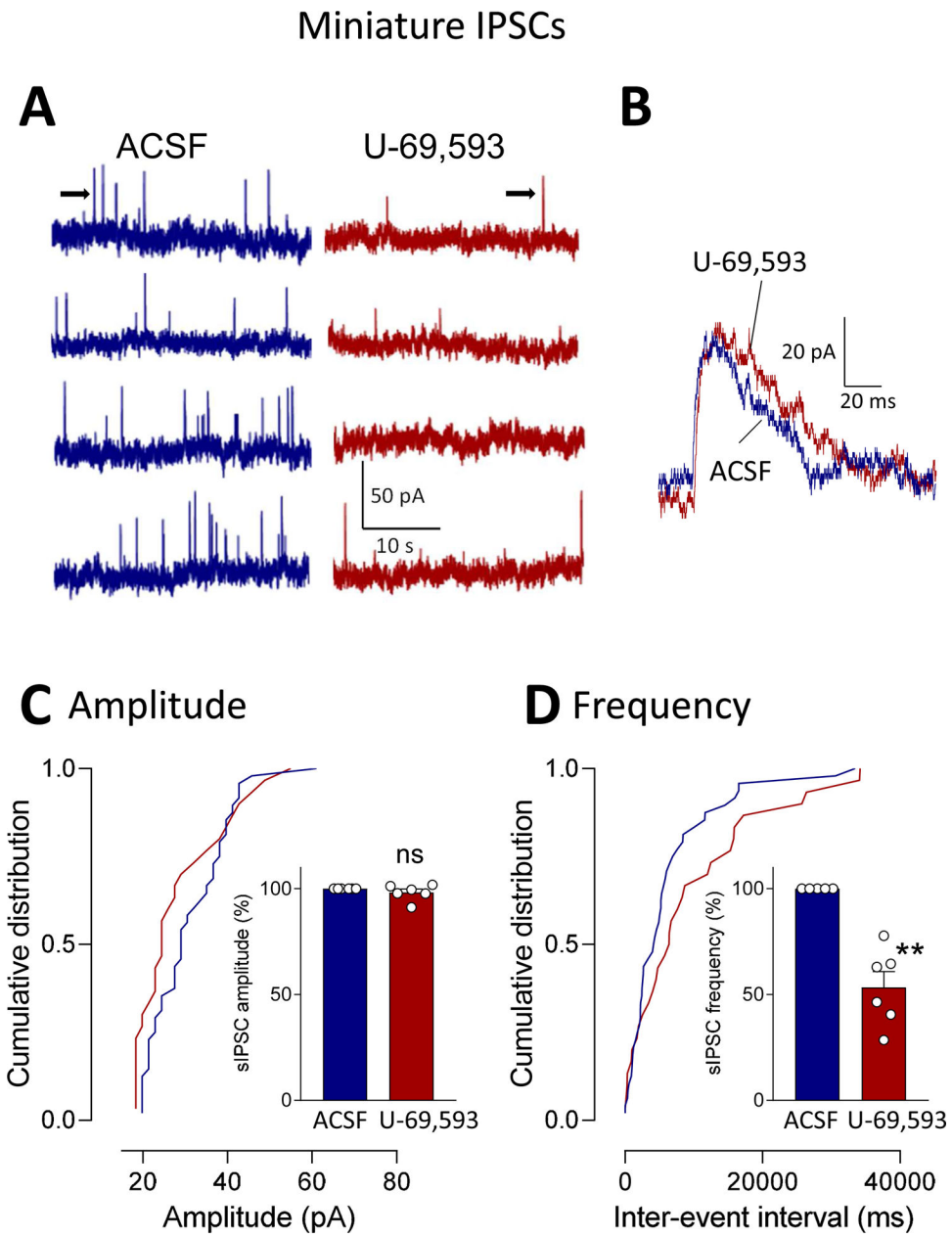

Figure 6. Effects of a KOR agonist (U-69,593) on miniature IPSCs (mIPSCs) in CeA-CRF neurons.

Whole-cell patch-clamp recordings were obtained from visually identified CeA-CRF neurons (see Materials and Methods). **(A)** Traces show individual examples of voltage-clamp recordings of mIPSCs during application of ACSF and U-69,593 (1 μM, 15 min). **(B)** Traces of individual mIPSCs (taken from traces in A as indicated by arrows) show that $GABA_A$ channel kinetics were not altered by U-69,593. **(C)** Analysis of cumulative distribution (individual neuron) and mean mIPSC amplitude showed that U-69,593 had no significant effect on amplitude (n = 6; P > 0.05, paired t-test, compared to ACSF predrug control). **(D)** U-69,593 decreased mIPSC frequency significantly (n = 6; P < 0.01, paired t-

test compared to predrug ACSF). Bar histograms show means ± SEM. Symbols show values of individual neurons.

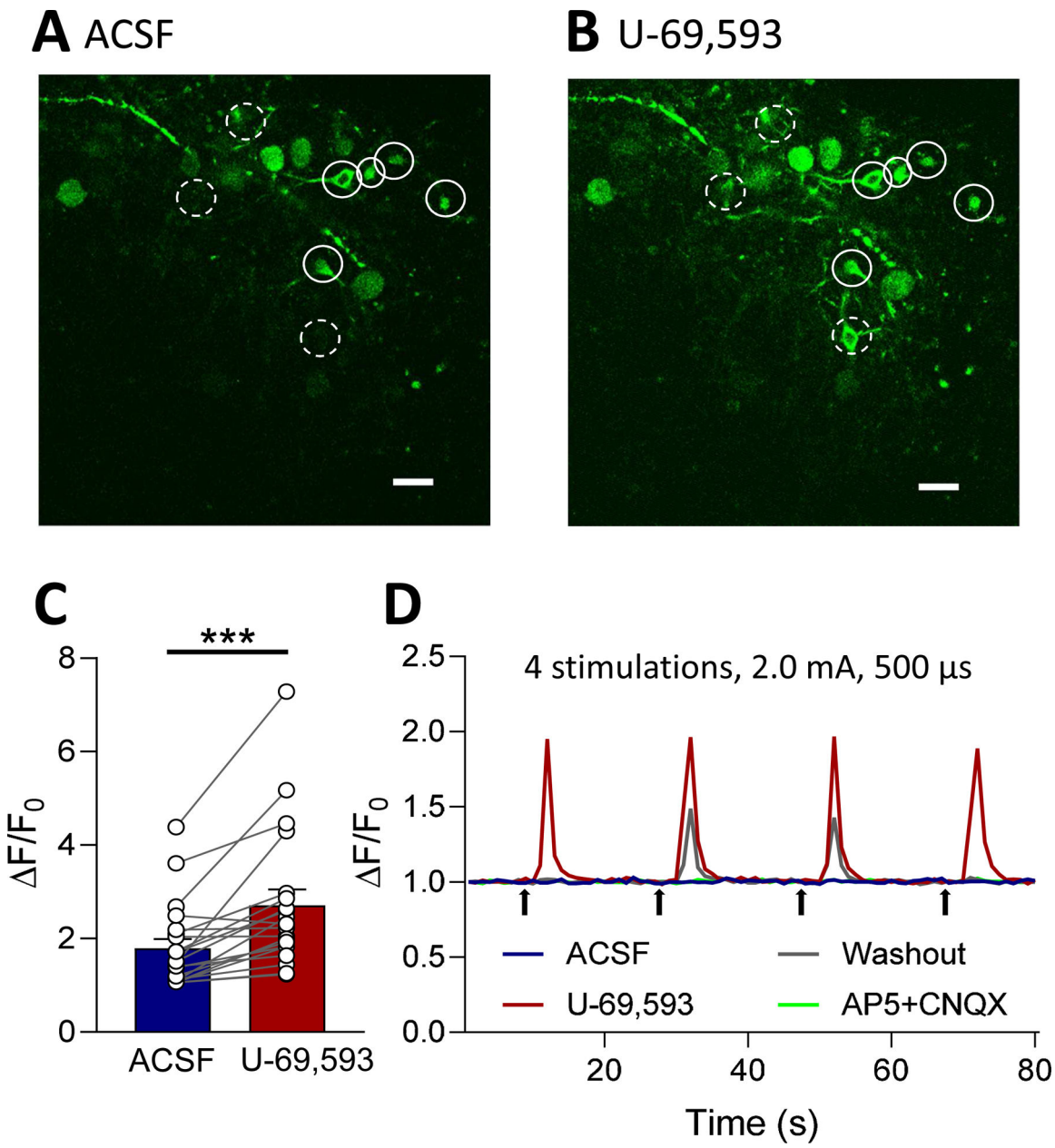

Figure 7. Effects of a KOR agonist (U-69,593) on calcium transients in CeA-CRF neurons.

Calcium imaging of CeA-CRF neurons in brain slices was done using a multiphoton system (see Materials and Methods). **(A, B)** Images show CeA-CRF neurons expressing a fluorescent calcium indicator (GCaMP6f) in response to electrical stimulation (2.0 mA, 0.5ms) of presumed parabrachial afferents (see Materials and Methods). Solid and dashed circles indicate neurons that fluoresced after application of U-69,593 (1 μM, 15 min; B) compared to the same neurons in the presence of vehicle (ACSF, A). **(C)** U-69,593 increased calcium transients in CeA-CRF neurons expressing GCaMP6f (n = 20 neurons, 4 rats; $P < 0.001$, paired t-test, compared to predrug control). **(D)** Traces show the responses of an individual CeA-CRF neuron during application of ACSF, U-69,593, washout in ACSF, and

AP5 (50uM) and CNQX (20uM). Bar histograms show means ± SEM. Symbols show values of individual neurons.